ORIGINAL PAPER

Theoretical study on the structures and properties of mixtures of urea and choline chloride

Hui Sun · Yan Li · Xue Wu · Guohui Li

Abstract In this work, we investigated in detail the structural characteristics of mixtures of choline chloride and urea with different urea contents by performing molecular dynamic (MD) simulations, and offer possible explanations for the low melting point of the eutectic mixture of choline chloride and urea with a ratio of 1:2. The insertion of urea molecules was found to change the density distribution of cations and anions around the given cations significantly, disrupting the long-range ordered structure of choline chloride. Moreover, with increasing urea concentration, the hydrogen bond interactions between choline cations and Cl⁻ anions decreased, while those among urea molecules obviously increased. From the hydrogen bond lifetimes, it was found that a ratio of 1:2 between choline chloride and urea is necessary for a reasonable strength of hydrogen bond interaction to maintain the low melting point of the mixture of choline chloride with urea. In addition, it was also deduced from the interaction energies that a urea content of 67.7 % may make the interactions of cation–anion, cation–urea and anion–urea modest, and thus results in the lower melting point of the eutectic mixture of choline chloride and urea. The present results may offer assistance to some extent for understanding the physicochemical properties of the eutectic mixture of choline chloride and urea, and give valuable information for the further development and application of deep eutectic solvents.

H. Sun · Y. Li · X. Wu · G. Li (✉)
Laboratory of Molecular Modeling and Design,
State key Laboratory of Molecular Reaction Dynamics,
Dalian Institute of Chemical Physics,
Chinese Academy of Sciences, 457 Zhongshan Rd.,
Dalian 116023, People's Republic of China
e-mail: ghli@dicp.ac.cn

Introduction

In the past decade, ionic liquids (ILs) have attracted more and more attention [1, 2]. They generally consist of organic cations and inorganic anions, and this special composition endows ILs with some "green" characteristics [3–6], such as negligible vapor pressure, excellent thermal and chemical stability, non-flammablility and good reusability. Thus, ILs have been branded as "environmentally friendly solvents and benign reaction media" [7–9]. However, with more thorough development of research on ILs, the potential environmental risks of ILs are being increasingly recognized [10–12]. So far, many ILs, such as the traditional imidazolium-based ILs, have been confirmed to possess toxicity and poor biodegradability, which brings environmental risks [10, 12]. Therefore, much attention is nowadays focused on developing new, more environmentally friendly ILs using renewable and non-toxic biosources.

In 2003, Abbott et al. [13] first reported that choline chloride could be mixed with urea at a ratio of 1:2 to form an eutectic mixture with a melting point of 12 °C. The eutectic mixture was found to have similar properties to ILs, such as low vapor pressure, powerful solvent capacity, high electrochemical conductivity, and so on. More particularly, many benefits that traditional ILs lack are also observed for the eutectic mixture. First, it consists of choline chloride and urea, which are natural and easily available feedstocks, and thus is an economical alternative to the traditional ILs. Next, it is sustainable and biodegradable, and hence is also an environmentally acceptable solvent instead of ILs. To differentiate it from ILs, the term deep eutectic solvent (DES) has been adopted. Up to now, many kinds of DESs have been reported, composed mostly of

substituted quaternary ammonium salts, e.g., choline chloride, and uncharged hydrogen bond donors such as amine, amide, carboxylic acid, and alcohol [14–16]. Meanwhile, these DESs have been applied widely as solvents and reaction mediums in many areas, including electrochemistry [17, 18], biochemistry [19–21] and material science [22], etc.

Although research on DESs has made great progress, an explicit and complete knowledge of the microstructures of DESs is still lacking, thus hindering our understanding of the properties of DESs, especially the very large depression of melting points of DESs (e.g., the melting points of choline chloride, urea and the corresponding eutectic mixture are 302, 133 and 12 °C, respectively). Therefore, great efforts should be made to investigate their structures, properties and structure–property relationships, through which valuable information will be obtained to guide the further development and application of DESs.

In this work, we consider choline chloride and urea as theoretical models (Scheme 1) to investigate the structures of mixtures of choline chloride and urea with different urea concentrations by performing molecular dynamic (MD) simulations. We arrive at a reasonable explanation for the low melting point of the eutectic mixture of choline chloride and urea with a ratio of 1:2. The present theoretical results are expected to yield valuable information for the further development and application of DESs.

Computational details and models

All MD simulations were carried out using the GROMACS 4.0.5 software package [23, 24]. The all-atom force field expanded by Lopes et al. [25–29] based on the OPLS-AA/AMBER framework was applied to choline chloride, where the charge values in the force field parameters were corrected by a factor of 0.9. In order to validate the reliability of the force field, we computed the densities for the mixtures of choline chloride and water with mass fraction of choline chloride at 10.0 % and 20.0 % under different pressures and temperatures, which were found to be in good agreement with the corresponding experimental values [30], as shown in Table 1. The parameters for urea were adopted from previous MD studies [31]. All simulations were performed in the isobaric-isothermal (NPT) ensemble with a pressure of 1 bar and a compressibility of $4.5 \times 10^{-5} bar^{-1}$. A leap-frog
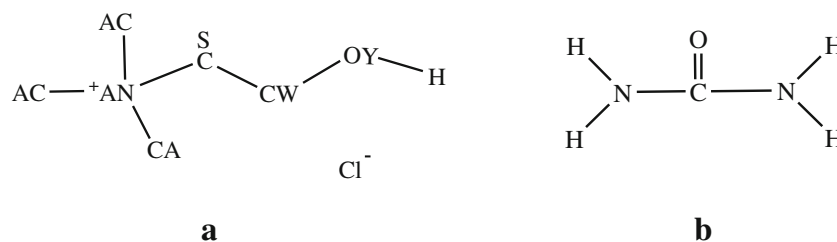
algorithm with a time step of 1 fs was used to integrate Newton's equations of motion. The cutoff distance of the neighbor searching was set to 1.2 nm, beyond which the long-range electrostatic interactions were computed using the particle mesh Ewald (PME) method [32, 33] with a grid spacing of 0.12 nm and fourth-order interpolation. Coulombic and Lennard-Jones interactions between atoms separated by three bonds were scaled by a factor of 0.5.

Six model systems with urea mole fraction from 0 to 100 % were established for the MD simulations on mixtures of choline chloride and urea. The sizes of the model systems are shown in Table 2. Initially, these cations, anions and urea molecules were scattered randomly in a low density cubic box with periodic boundary conditions. After energy minimization using the steepest descent method, the volume of the box was compressed to a normal value by performing a 1 ns simulation in NPT ensemble. The resulting configuration was used for the subsequent equilibrium run. In order to obtain a better equilibrium structure, our simulations in the equilibrium stage were first carried out at a much higher temperature, 600 K. The final configuration of 600 K was then sequentially cooled down to 285 K after a series of decreased temperatures, i.e., 500 and 400 K. In each case, the trajectory was run for a duration of 2 ns, using a Berendsen thermostat/barostat algorithm [34], and the final configuration obtained was used as the starting point for the next simulation at the subsequent lower temperature. After equilibration, the target temperature was set to 285 K, which was the melting point of the eutectic mixture of choline chloride and urea with a ratio of 1:2. At the target temperature, a simulation of 25 ns was first carried out for equilibrium, and then extended by an additional 5 ns for the production run, in which data were collected every 0.1 ps for analysis. In the production stage, temperature and pressure were scaled with Nose-hoover thermostat [35] and Parrinello-Rahman barostat [36], whose coupling time constants were 0.5 and 2.0 ps, respectively.

Results and discussion

Radial distribution function analysis

The radial distribution functions (RDFs), also called pair correlation functions, were first calculated to analyze the

Scheme 1 Schematic structures and main atom type notations of **a** choline chloride and **b** urea

a   **b**

Table 1 Comparison of experimental and calculated densities

State point	T(K)	P(bar)	[Choline][Cl] (wt%)	$\rho(\text{g cm}^{-3})$		Percentage difference
				Simulation	Experiment	
1	298.0	1.0	20.0	1.060	1.021	3.82
2	305.0	10.0	10.0	1.044	1.007	3.67

probability distributions of cations, anions or urea molecules around the given cations or urea molecules at a certain distance, where the geometric centers of NA, CS and CW atoms in the choline cation and the C atom in the urea molecule were taken as the positions of choline cation and urea molecule. The corresponding calculated results are shown in Fig. 1.

The cation–anion RDF for pure choline chloride, as shown by $g(r)_{ca}$, shows a first maximum at 0.450 nm, while the first maximum peak of the $g(r)_{cc}$ for pure choline chloride appears at a distance of about 0.638 nm, which is farther than that of the $g(r)_{ca}$ and is in a similar position to the minima of $g(r)_{ca}$, implying that pure choline chloride presents an ordered structure with alternately arranged cations and anions. With increasing urea concentration, values corresponding to the first maximum peak positions of the cation–anion and cation–cation RDFs gradually increase, and the first peaks of the cation–cation RDFs are observed to gradually split into two peaks. These results indicate that the insertion of urea molecules changes significantly the probability distribution of cations around the given cations and decreases the interactions between cations and anions/cations. Moreover, $g(r)_{ca}$ and $g(r)_{cc}$ exhibit strong and damped oscillations in pure choline chloride, indicating long-range spatial correlation between ions and ions, which is in line with the common characteristic of strongly coupled ionic systems [37]. However, with increasing urea concentration, the oscillation amplitudes of $g(r)_{ca}$ and $g(r)_{cc}$ gradually fade, implying that the long-range ordered structure of choline chloride is disrupted after addition of urea molecules.

Subsequently, we analyzed the probability distributions of anions or urea molecules around the given cations or urea molecules at a certain distance. The first maximum peaks of $g(r)_{cu}$ are located at 0.480–0.496 nm, i.e., longer than the distances of the first maximum peaks of $g(r)_{ca}$ (0.450–0.482 nm), but shorter than those of $g(r)_{cc}$ (0.638–0.648 nm). These results confirm that the urea molecules

enter into the second layer around the given cations, and interact mainly with Cl$^-$ anions. Compared with $g(r)_{ca}$ and $g(r)_{cc}$, the values corresponding to the first maximum peak positions of $g(r)_{ua}$, $g(r)_{cu}$ and $g(r)_{uu}$ decrease slightly as the urea content increases, indicating the interactions between cations, anions, urea molecules and urea molecules are enhanced.

It should be noted that, in most RDF figures, the long-range behavior is quite noisy and bumpy. In order to address this issue, the size of the simulation box and the sampling time for data collection, respectively, were checked. The box sizes are shown in Table 2, and were found to be reasonable, with sizes similar to the boxes used in other simulated systems of ILs [38–40]. Furthermore, the RDFs were recalculated on a longer sampling time; the results are shown in Figure S1. It can be observed that the RDF profiles in Figure S1 are in good agreement with those in Fig. 1. Therefore, the noisiness and bumpiness of RDFs are due to neither too small a simulation box or too short a sampling time, but rather the insertion of urea molecules. This can be observed by comparing the RDFs in pure choline chloride and pure urea with the corresponding RDFs in the mixtures of choline chloride and urea.

Spatial distribution function analysis

To visualize the cation, anion and urea distributions around a given cation, as well as the anion distributions around a given urea molecule, the views of the corresponding spatial distribution functions (SDF) were plotted (Fig. 2). As shown by the isosurface $\mathbf{I}_{a\text{-}e}$, the three-dimensional density distribution of anions around cations is seen vividly. It was found that Cl$^-$ anions prefer to be positioned near the H atoms associating with the OY and CA atoms of the cation. This can be attributed to the larger electronegativity of the OY atom and the greater positive charge gathered on the NA atom, which make the H atoms associate with the OY and

Table 2 Sizes for different simulated systems

		Mole % Urea					
		0.0	25.0	50.0	67.7	75.0	100.0
Molecule Numbers	N_{IL}	198	198	198	198	198	0
	N_{Urea}	0	66	198	415	594	594
Box length (Å)		35.0	36.2	38.3	41.4	43.6	34.7
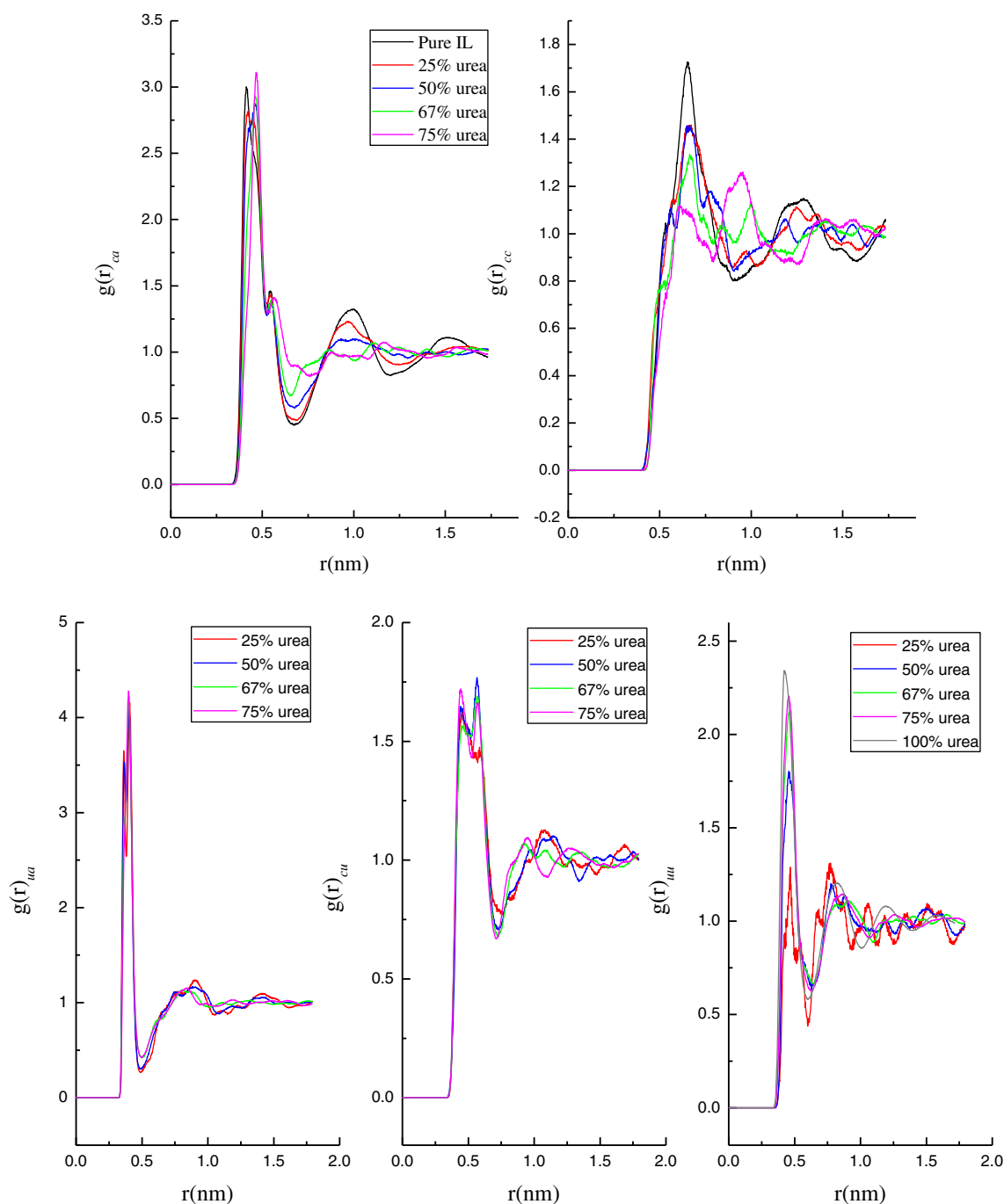
Fig. 1 Radial distribution functions (RDFs) for cation–cation $g(r)_{cc}$, cation–anion $g(r)_{ca}$, urea–anion $g(r)_{ua}$, cation–urea $g(r)_{cu}$ and urea–urea $g(r)_{uu}$

CA atoms, bringing more positive charge. With increasing urea concentration, the density distribution of anions near the H atoms associating with the CA atom of the cation gradually diminish. The density distribution of cations around the given cation can be obtained from isosurfaces II_{a-e} in Fig. 2,. Clearly, the cations center mainly on the next available space that is not occupied by anions in the first coordinate shell around the given cation (for details, see Fig. S2), which are quite favorable for the formation of a

hydrogen bond network between cations and anions. Moreover, the increase in urea content makes the distribution of cations around the given cation become very disordered, and move farther from the given cation, as shown by II_e. The different positions of cations around the given cation result in the split of the first maximum peak of the $g(r)_{cc}$ observed above. The results indicate that significant rearrangement of anions and cations takes place in order to accommodate urea molecules.
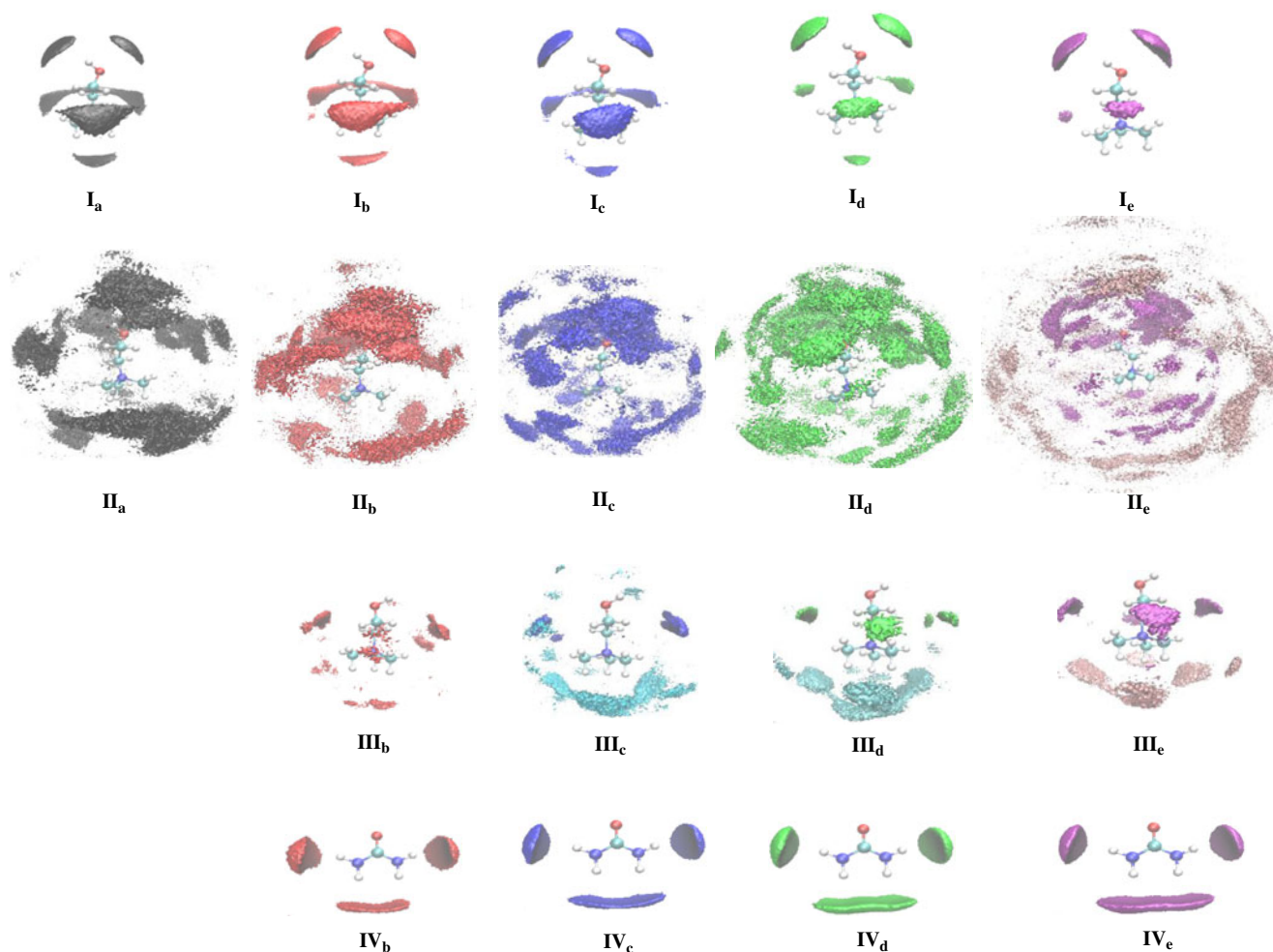
Fig. 2 Colored spatial distribution functions (SDFs) for (*I*) anions around cations, (*II*) cations around cations, (*III*) ureas around cations and (*IV*) anions around ureas, respectively, where subscripts *a–e* stand for the mole fraction of urea, i.e., 0.0 %, 25.0 %, 50.0 %, 67.7 % and 75.0 %

Subsequently, the density distributions of urea molecules around the given cation and Cl^- anions around the given urea molecule were also investigated. As depicted by **III**$_{b-e}$, the urea molecules are located mainly near the H atoms associating with the CA atom of the cation, and the density distribution increases as the urea concentration enhances, which offers a reasonable explanation for the decrease in density distribution of anions near the H atoms associating with the CA atom of the cation. Finally, it was observed that the density distribution of Cl^- anions around the given urea molecule barely changed over the whole concentration range, which is mainly close to the H atoms in urea molecules, as exhibited by **IV**$_{b-e}$.

Through the RDF and SDF analyses, it is found that pure choline chloride shows a strong long-range ordered structure with cations and anions arranged alternately. However, with the increase in urea concentration, significant rearrangement for anions and cations takes place in order to accommodate urea molecules, and thus the interaction between anions and cations decreases, which may result in a

low melting point for the eutectic mixture of choline chloride and urea with a ratio of 1:2 (i.e., the mole percent of urea is 67.7 %).

Hydrogen bond analysis

In order to better understand the structures for the mixtures of urea and choline chloride, and to offer a reasonable explanation for the low melting point of the eutectic mixture containing 67.7 % urea, we analyzed the hydrogen bonds by examining the site–site RDFs between the H atoms of choline cations and Cl^- anions or the negatively charged O atoms of urea molecules. The results are shown in Figs. 3 and 4, respectively.

The first maximum peaks for the RDFs between the H atoms of choline cations and Cl^- anions are located near 0.280 nm for the CA-H···Cl pair, 0.286 nm for the CS-H···Cl pair, 0.308 nm for the CW-H···Cl pair, and 0.192 nm for the OY-H···Cl pair. Among these distances, those for the CA-H···Cl, CS-H···Cl and OY-H···Cl pairs are less than the
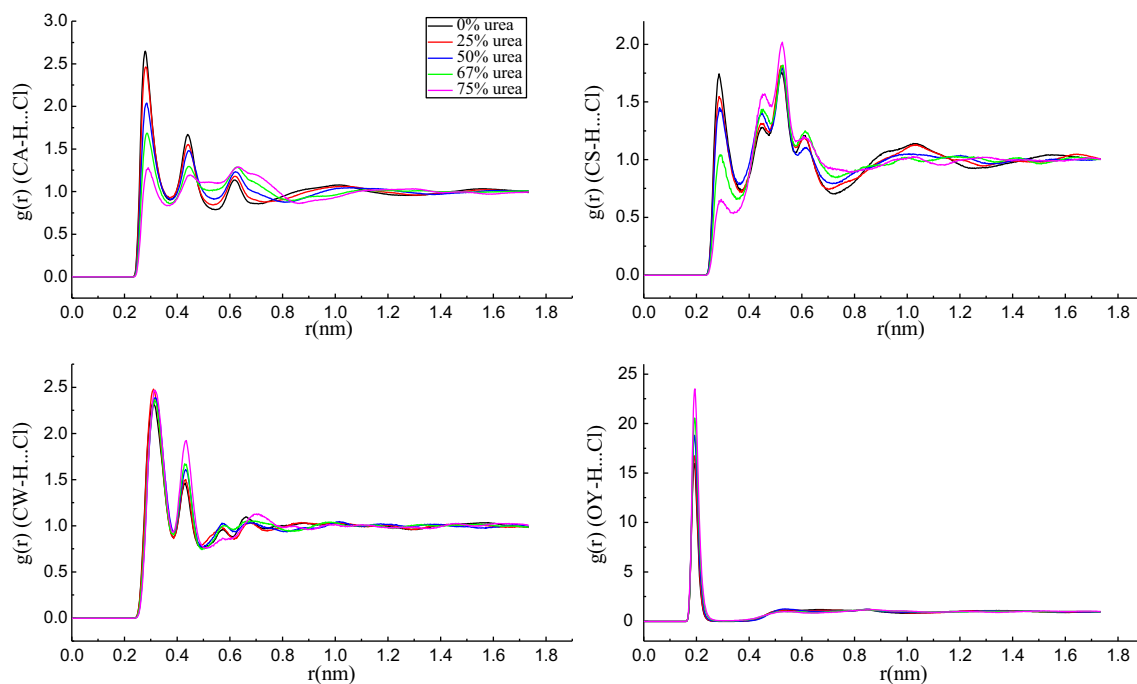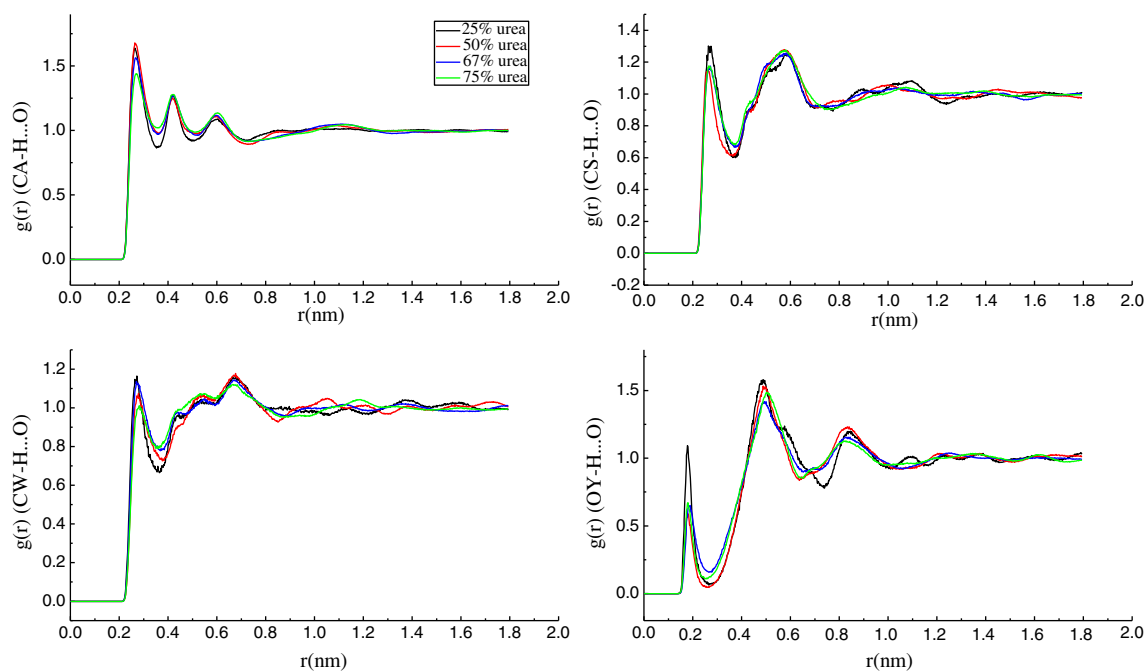
Fig. 3 Site–site RDFs of Cl⁻ anion with H atoms on the choline cations

sum (0.295 nm) of the van der Waals radii of H and Cl atoms, which represent the most likely hydrogen bond distances. As can be judged from the hydrogen bond distances, the OY-H···Cl hydrogen bond is strongest, which can be attributed to the larger electronegativity of the OY atom. In addition, with increasing the urea concentration, the first maximum peak intensities of CA-H···Cl and CS-H···Cl

obviously decrease, while those of OY-H···Cl increase slightly. This is in good agreement with results obtained from SDF analysis, in which it was observed that Cl⁻ anions preferred to be positioned near H atoms associating with OY and CA atoms; however, an increase in urea concentration leads to the gradual disappearance of the density distribution of anions around H atoms associating with CA atoms.

Fig. 4 Site-site RDFs of O atoms of urea molecules with H atoms on the choline cations

Figure 4 shows the site–site RDFs between the H atoms of choline cations and the negatively charged O atoms of urea molecules. The corresponding first maximum peaks are located near 0.264 nm for the CA-H···O pair, 0.264 nm for the CS-H···O pair, 0.272 nm for the CW-H···O pair, and 0.488 nm for the OY-H···O pair. According to the sum (0.272 nm) of the van der Waals radii of H and O atoms, it was deduced that the CA-H···O and CS-H···O interactions with distances of 0.264 nm belong to hydrogen bond interactions, and the hydrogen bonds are less intense than the OY-H···Cl interaction. As the urea concentration increases, only small changes are observed for the CA-H···O and CS-H···O intensity, which are slightly weakened. It should be noted that the RDF for OY-H···O pair shows small peaks at about 0.178 nm; however, with increasing urea concentration, the small peak intensity clearly decreases, implying a decreased probability of the appearance of urea molecules around the H atoms connecting with the OY atom. This is in line with results from the SDF analysis.

In order to understand the interactions between urea molecules and Cl⁻ anions or urea molecules, the site–site RDFs of H atoms on urea molecules with Cl⁻ anions or the negatively charged O atoms of urea molecules were also investigated. The results are shown in Fig. 5. The first maximum peaks for N-H···Cl and N-H···O pairs appear at distances of about 0.210 and 0.192 nm, i.e., less than the sums (0.295 and 0.272 nm) of the van der Waals radiis of H and Cl/O atoms, which indicates the formation of N-H···Cl and N-H···O hydrogen bonds. It should be noted that the first maximum peak intensities for N-H···Cl interactions are much greater than those of CA-H···O and CS-H···O interactions, which implies that urea molecules interact mainly with Cl⁻ anions in the mixtures of choline chloride with urea, in good agreement with the above RDF analysis. In addition, as urea content increases, the first maximum peak intensities for N-H···Cl interactions decrease slightly, and those for N-H···O interactions obviously increase.

In short, it is concluded from the above analysis that urea molecules interact mainly with Cl⁻ anions through N-H···Cl hydrogen bonds in the mixtures of choline chloride with urea, which is the leading cause of the decrease in hydrogen bond interactions between choline cations and Cl⁻ anions, and thus induces the decline of the melting point of choline chloride. Meanwhile, an important point to note is that the hydrogen bond interactions among urea molecules obviously increase with increasing urea content, which again will result in the increase of the melting point for the mixtures of choline chloride with urea. Therefore, we consider that an appropriate ratio between choline chloride and urea is needed for a reasonable strength of hydrogen bond interaction to maintain the low melting point of the mixtures of choline chloride with urea.

Finally, to monitor the persistence of specific hydrogen bonds, the lifetimes of relatively strong OY-H···Cl, N-H···Cl and N-H···O hydrogen bonds were measured using the rectified g_hbond analysis tool implemented in GROMACS, where the acceptor-donor distance criterion is 0.295 and 0.272 nm for H···Cl and H···O interactions, and the hydrogen-donor-acceptor angle criterion is taken from 0 to 30°. The calculated lifetimes are listed in Table 3. An interesting phenomenon that can be observed from Table 3 that the eutectic mixture containing 67.7 % urea has relatively shorter lifetimes for OY-H···Cl, N-H···Cl and N-H···O hydrogen bonds, implying that the movements of particles are freer in the eutectic mixture containing 67.7 % urea, and thus results in the low melting point of the eutectic mixture of choline chloride and urea with a ratio of 1:2.

**Fig. 5** Site–site RDFs of Cl⁻ anions and O atoms of urea molecules with H atoms on the urea molecules
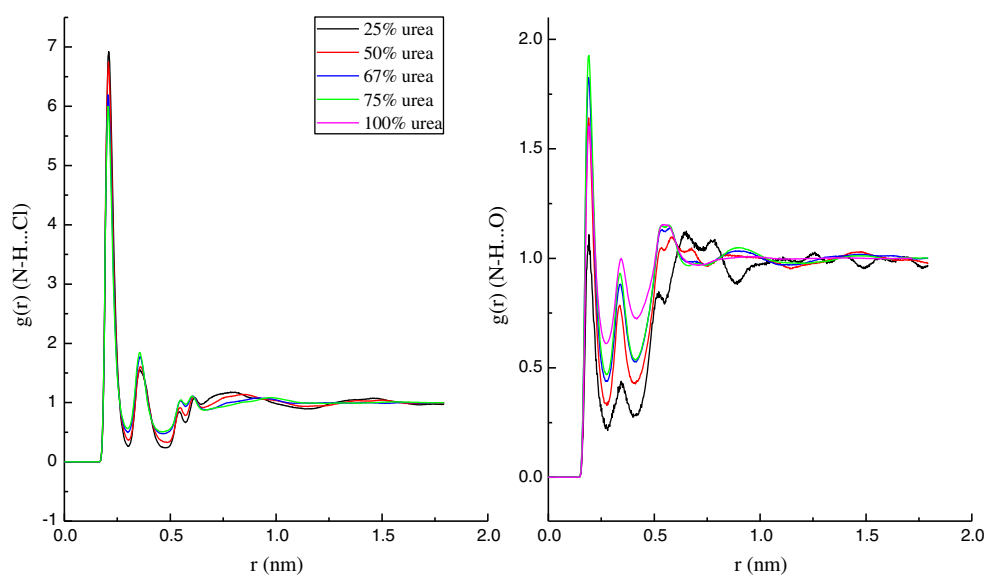
Table 3 Lifetimes (ps) of hydrogen bonds[a]

	Mole % urea				
	0.0	25.0	50.0	67.7	75.0
OY-H···Cl	18.800	18.443	12.319	12.574	16.346
N-H···Cl	——	4.547	2.810	2.397	4.062
N-H···O	——	14.658	3.947	2.952	4.300

[a] To determine the hydrogen bonds, the acceptor-donor distance criterion is 0.295 and 0.272 nm for H···Cl and H···O interactions, the hydrogen-donor-acceptor angle criterion is taken from 0 to 30°

Interaction energy analysis

It is well known that the melting point is also related to the interaction energies of cation–anion, cation–urea and anion–urea, which can be calculated by the addition of the corresponding van der Waals and electrostatic interaction energies. The energy terms were extracted from the trajectories using the g_energy analysis tool in the GROMACS package. The calculated results are shown in Fig. 6. It is clear that the interaction between anions and urea molecules is stronger than that between cations and urea molecules, indicating that urea molecules interact mainly with Cl^- anion, which is consistent with the results from the above RDF and hydrogen bond analyses. Furthermore, the interaction energies between cations and anions are larger than those between cations or anions and urea molecules with the mole fraction of urea at 0–50.0 %. When the content of urea rises to 67.7 %, the interaction between urea molecules and anions is stronger than that of cations with anions, and as the urea content increases still further, this trend is more evident. Therefore, it is deduced that a urea content of 67.7 % could make the cation–anion, cation–urea and anion–urea interactions more modest, thus resulting in the lower
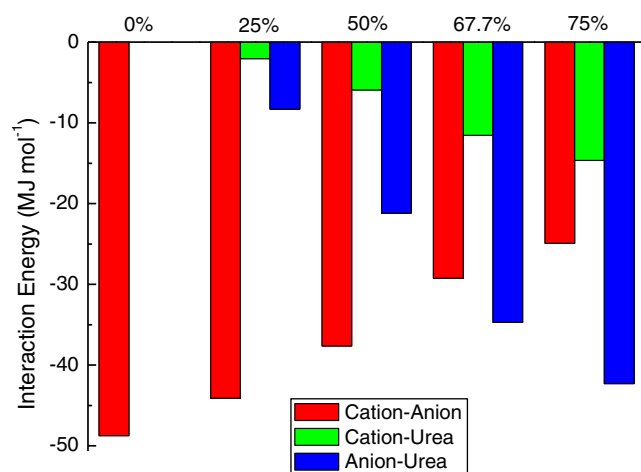
Fig. 6 Interaction energies of cation–anion, cation–urea and anion–urea

melting point of the eutectic mixture of choline chloride and urea.

Conclusions

In this paper, we report a detailed investigation using MD simulations of the structural characteristics of mixtures of choline chloride and urea with different urea concentrations; the results give a reasonable explanation for the low melting point of the eutectic mixture of choline chloride and urea with a ratio of 1:2.

MD simulation on pure choline chloride represents a strong long-range ordered structure with cations and anions arranged alternately. Cl^- anions prefer to interact with the H atoms associating with OY and CA atoms of cations through hydrogen bonds, and the cations center mainly on the next available space that is not occupied by anions in the first coordinate shell around the given cation. In mixtures of choline chloride and urea, the urea molecules enter the second layer around the given cations, and appear near the H atoms associating with the CA atom of the cation to interact mainly with Cl^- anions. Therefore, in order to accommodate urea molecules, most Cl^- anions are positioned near H atoms associating with OY atoms of cations, while the density distribution of cations around the given cation becomes very disordered, and moves farther from the given cation, which disrupts the long-range ordered structure of choline chloride. With the increase in urea concentration, the hydrogen bond interactions between choline cations and Cl^- anions decrease, while those among urea molecules obviously increase. From the lifetimes of the relatively strong OY-H···Cl, N-H···Cl and N-H···O hydrogen bonds, it was found that a ratio of 1:2 between choline chloride and urea is necessary for a reasonable strength of hydrogen bond interaction to maintain the low melting point of the mixtures of choline chloride with urea. In addition, it was deduced from the interaction energies that a urea content of 67.7 % may make the interactions of cation–anion, cation–urea and anion–urea more modest, and thus result in the lower melting point of the eutectic mixture of choline chloride and urea.

The present results show some structural details of the mixtures of choline chloride and urea with different urea concentrations, which may offer assistance to some extent for understanding the physicochemical properties of the eutectic mixture of choline chloride and urea, and give valuable information for the further development and application of DESs.

References

1. Endres F, Abedin SZE (2006) Air and water stable ionic liquids in physical chemistry. Phys Chem Chem Phys 8:2101–2116
2. Wishart JF, Castner EW Jr (2007) The physical chemistry of ionic liquids. J Phys Chem B 111:4639–4640
3. Seddon KR (1997) Ionic liquids for clean technology. J Chem Technol Biotechnol 68:351–356
4. Wasserscheid P, Welton T (eds) (2003) Ionic liquids in synthesis. Wiley-VCH, Weinheim
5. Chiappe C, Pieraccini D (2005) Ionic liquids: solvent properties and organic reactivity. J Phys Org Chem 18:275–297
6. Ranke J, Stolte S, Störmann R, Arning J, Jastorff B (2007) Design of sustainable chemical products—the example of ionic liquids. Chem Rev 107:2183–2206
7. Welton T (1999) Room-temperature ionic liquids. Solvents for synthesis and catalysis. Chem Rev 99:2071–2083
8. Sheldon R (2001) Catalytic reactions in ionic liquids. Chem Commun 23:2399–2407
9. Bourbigou HO, Magna L (2002) Ionic liquids: perspectives for organic and catalytic reactions. J Mol Catal A 182–183:419–437
10. Wells AS, Coombe VT (2006) On the freshwater ecotoxicity and biodegradation properties of some common ionic liquids. Org Process Res Dev 10:794–798
11. Nockemann P, Thijs B, Driesen K, Janssen CR, Hecke KV, Meervelt LV, Kossmann S, Kirchner B, Binnemans K (2007) Choline saccharinate and choline acesulfamate: ionic liquids with low toxicities. J Phys Chem B 111:5254–5263
12. Romero A, Santos A, Tojo J, Rodríguez A (2008) Toxicity and biodegradability of imidazolium ionic liquids. J Hazard Mater 151:268–273
13. Abbott AP, Capper G, Davies DL, Rasheed RK, Tambyrajah V (2003) Novel solvent properties of choline chloride/urea mixtures. Chem Commun 2003:70–71
14. Abbott AP, Boothby D, Capper G, Davies DL, Rasheed RK (2004) Deep eutectic solvents formed between choline chloride and carboxylic acids: versatile alternatives to ionic liquids. J Am Chem Soc 126:9142–9147
15. Kareem MA, Mjalli FS, Hashim MA, AlNashef IM (2010) Phosphonium-based ionic liquids analogues and their physical properties. J Chem Eng Data 55:4632–4637
16. Abbott AP, Capper G, Gray S (2006) Design of improved deep eutectic solvents using hole theory. ChemPhysChem 7:803–806
17. Zhao C, Burrell G, Torriero AAJ, Separovic F, Dunlop NF, MacFarlane DR, Bond AM (2008) Electrochemistry of room temperature protic ionic liquids. J Phys Chem B 112:6923–6936
18. Nkuku CA, LeSuer RJ (2007) Electrochemistry in deep eutectic solvents. J Phys Chem B 111:13271–13277
19. Gorke, JT, Srienc F, Kazlauskas RJ (2008) Hydrolase-catalyzed biotransformations in deep eutectic solvents. Chem Commun 1235–1237
20. Lindberg D, Revenga MDLF, Widersten M (2010) Deep eutectic solvents (DESs) are viable cosolvents for enzyme-catalyzed. J Biotechnol 147:169–171
21. María PDD, Maugeri Z (2011) Ionic liquids in biotransformations: from proof-of-concept to emerging deep-eutectic-solvents. Curr Opin Chem Biol 15:220–225
22. Zhang J, Wu T, Chen S, Feng PY, Bu XH (2009) Versatile structure-directing roles of deep-eutectic solvents and their implication in the generation of porosity and open metal sites for gas storage. Angew Chem Int Ed 48:3486–3490
23. Berendsen HJC, van der Spoel D, van Drunen R (1995) GROMACS: a message-passing parallel molecular dynamics implementation. Comput Phys Commun 91:43–56
24. Van Der Spoel D, Lindahl E, Hess B, Groenhof G, Mark AE, Berendsen HJ (2005) GROMACS: Fast, flexible, and free. J Comput Chem 26:1701–1718
25. Lopes JNC, Deschamps J, Pádua AAH (2004) Modeling ionic liquids using a systematic all-atom force field. J Phys Chem B 108:2038–2047
26. Lopes JNC, Deschamps J, Pádua AAH (2004) Modeling ionic liquids using a systematic all-atom force field. (Addition/Correction). J Phys Chem B 108:11250
27. Lopes JNC, Pádua AAH (2004) Molecular force field for ionic liquids composed of triflate or bistriflylimide. J Phys Chem B 108:16893–16898
28. Lopes JNC, Pádua AAH (2006) Using spectroscopic data on imidazolium cation conformations to test a molecular force field for ionic liquids. J Phys Chem B 110:7485–7489
29. Lopes JNC, Pádua AAH (2006) Molecular force field for ionic liquids III: imidazolium, pyridinium, and phosphonium cations; chloride, bromide, and dicyanamide anions. J Phys Chem B 110:19586–19592
30. Rowley RL (1994) Statistical mechanics for thermophysical property calculations. Prentice-Hall, New York
31. Duffy EM, Severance DL, Jorgensen WL (1993) Urea: potential functions, log P, and free energy of hydration. Isr J Chem 33:323
32. Darden T, York D, Pedersen L (1993) Particle mesh Ewald: an N-log(N) method for Ewald sums in large systems. J Chem Phys 98:10089–10092
33. Essmann U, Perera L, Berkowitz ML, Darden T, Lee H, Pedersen LG (1995) A smooth particle mesh Ewald method. J Chem Phys 103:8577–8593
34. Berendsen HJC, Postma JPM, van Gunsteren WF, DiNola A, Haak JR (1984) Molecular dynamics with coupling to an external bath. J Chem Phys 81:3684–3690
35. Hoover W (1985) Canonical dynamics: equilibrium phase-space distributions. Phys Rev A 31:1695–1697
36. Parrinello M, Rahman A (1981) Polymorphic transitions in single crystals: a new molecular dynamics method. J Appl Phys 52:7182–7190
37. Keblinski P, Eggebrecht J, Wolf D, Phillpot SR (2000) Molecular dynamics study of screening in ionic fluids. J Chem Phys 113:282–291
38. Hanke CG, Lynden-Bell RM (2003) A simulation study of water-dialkylimidazolium ionic liquid mixtures. J Phys Chem B 107:10873–10878
39. Wu X, Liu Z, Huang S, Wang W (2005) Molecular dynamics simulation of room-temperature ionic liquid mixture of [bmim][BF$_4$] and acetonitrile by a refined force field. Phys Chem Chem Phys 7:2771–2779
40. Jiang W, Wang Y, Voth GA (2007) Molecular dynamics simulation of nanostructural organization in ionic liquid/water mixtures. J Phys Chem B 111:4812–4818